AIP Advances

Impact of artificial lateral quantum confinement on exciton-spin relaxation in a two-dimensional GaAs electronic system

Takayuki Kiba, Toru Tanaka, Yosuke Tamura, Akio Higo, Cedric Thomas, Seiji Samukawa, and Akihiro Murayama

Citation: AIP Advances **4**, 107112 (2014); doi: 10.1063/1.4897958
View online: http://dx.doi.org/10.1063/1.4897958
View Table of Contents: http://scitation.aip.org/content/aip/journal/adva/4/10?ver=pdfcov
Published by the AIP Publishing

Impact of artificial lateral quantum confinement on exciton-spin relaxation in a two-dimensional GaAs electronic system

Takayuki Kiba,[1,4,a] Toru Tanaka,[1] Yosuke Tamura,[2] Akio Higo,[3] Cedric Thomas,[2,4] Seiji Samukawa,[2,3,4] and Akihiro Murayama[1,4]
[1]*Graduate School of Information Science and Technology, Hokkaido University, Kita 14, Nishi 9, Kita-ku, Sapporo, Japan*
[2]*Institute of Fluid Science, Tohoku University, 2-1-1 Katahira, Aoba-ku, Sendai, Japan*
[3]*WPI-AIMR, Tohoku University, 2-1-1 Katahira, Aoba-ku, Sendai, Japan*
[4]*CREST Japan Science and Technology Agency, 5 Sanbancho, Chiyoda-ku, Tokyo, Japan*

(Received 22 May 2014; accepted 1 October 2014; published online 8 October 2014)

We demonstrate the effect of artificial lateral quantum confinement on exciton-spin relaxation in a GaAs electronic system. GaAs nanodisks (NDs) were fabricated from a quantum well (QW) by top-down nanotechnology using neutral-beam etching aided by protein-engineered bio-nano-templates. The exciton-spin relaxation time was 1.4 ns due to ND formation, significantly extended compared to 0.44 ns for the original QW, which is attributed to weakening of the hole-state mixing in addition to freezing of the carrier momentum. The temperature dependence of the spin-relaxation time depends on the ND thickness, reflecting the degree of quantum confinement. [http://dx.doi.org/10.1063/1.4897958]

Electronic spin states in semiconductor quantum structures such as quantum wells (QWs) and quantum dots (QDs) have provoked a great deal of controversy because of their potential applications to spin-functional electronic or photonic devices and quantum information processing, in addition to being of fundamental scientific interest.[1–5] Understanding the relaxation phenomena of the spin states of carriers or excitons is essential for determining the spin functionalities, because the spin information created and stored in these semiconductor quantum structures will be dissipated by the spin relaxation. It is well known that the spin-relaxation times of electrons, heavy holes (hhs), and excitons in the self-assembled QDs of compound semiconductors, such as InAs,[6] InGaAs,[7] CdSe,[8,9] and CdTe,[10] are significantly longer than those in two- or three-dimensional electronic systems such as QWs.[11–15] Therefore, a better and more comprehensive understanding of the effects of lateral quantum confinement of carriers or excitons on the spin-relaxation mechanism, in the absence of strong influences from complicated shapes and/or interfacial chemical states, is necessary for stabilization of the spin states in semiconductor QDs. One efficient way to study the spin-relaxation mechanism is to prepare intentionally tailored nanostructures directly fabricated from a QW without defects or shape anisotropies.

Our research group has recently constructed artificial GaAs nanodisks (NDs) with lateral diameters of less than 20 nm that exhibit strong quantum-confinement effects on carriers or excitons in lateral directions.[16–18] These NDs were directly fabricated from GaAs QWs by newly developed top-down lithography using ultra-low-damage neutral-beam etching[19] aided by protein-engineered bio-nano-templates of ferritin supramolecules.[20] These unique NDs provide us with the first good opportunity for quantitative testing of the effects of strong lateral quantum confinement on spin-relaxation dynamics.

[a]E-mail: tkiba@ist.hokudai.ac.jp

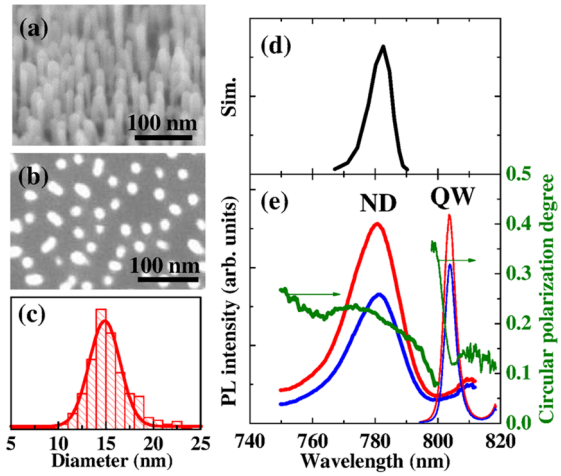

FIG. 1. (a) Tilted and (b) top views of the SEM image of the nanoscale pillars containing disk-shaped GaAs NDs. (c) The lateral diameter distribution; note that the elongated ellipsoidal images that had an aspect ratio between the major and minor axes smaller than 0.7 were not included because those pillars collapsed during the preparation of the sample for the SEM observation. (d) The calculated exciton-PL spectrum of the GaAs-ND ensemble based on the ND size distribution shown in (c). (e) Circularly polarized PL spectra at 6 K from the GaAs NDs (thick solid lines) and the original QW prior to etching (thin solid lines), under σ^+-polarized pulsed excitation resonant with the band edge energy of the $Al_{0.15}Ga_{0.85}As$ barrier (red lines: σ^+, blue lines: σ^-). The corresponding degrees of circular polarization (CPD) of the PL as a function of wavelength are also plotted (green lines). The PL intensities were time integrated over 0-1 ns after the pulsed excitation.

Details of the preparation of GaAs ND samples have been provided elsewhere.[16,17] First, double-layered QWs of GaAs/$Al_{0.15}Ga_{0.85}As$ with GaAs-well thicknesses of 8 and 4 nm were grown on GaAs (100) substrates using metal-organic vapor phase epitaxy (MOVPE). The surface was coated with ferritin supramolecules containing iron nanoparticles in their cavities. The average center-to-center distance of the dispersive ferritin molecules was 45 nm, which was also intentionally designed using the PEGylated ferritin.[21] The iron particles remaining after removal of the ferritin protein shells by ashing were then used as an etching mask for a subsequent etching process. As a result of neutral-beam etching, nanoscale pillars containing a disk-shaped QW section, i.e., a GaAs ND, were fabricated successively. Scanning electron microscope (SEM) images of the nanopillars with the GaAs NDs taken just after the neutral-beam etching are shown in Figs. 1(a) and 1(b). The distribution of the lateral diameters is plotted as an inset of Fig. 1(c). The average diameter is 15 nm and the distribution of the lateral sizes, ranging from 10 to 20 nm, can be expressed by a Gaussian function, as indicated by the solid line. Finally, $Al_{0.15}Ga_{0.85}As$ passivation, barrier layer and GaAs capping layer were re-grown by MOVPE. Therefore, the GaAs NDs were fully embedded in the layered barrier structure.

Detection of time-resolved and circularly polarized photoluminescence (PL) from the NDs was used to optically observe the spin-relaxation phenomena. A mode-locked Ti:Sapphire laser with a wavelength of 728 nm and a temporal width of 150 fs were used to produce pulsed excitation resonant with the band-gap energy of the barrier. The time-resolved, circularly polarized PL spectra were recorded using a streak camera.

Circularly polarized PL spectra from the GaAs NDs with the thickness of 8 nm at 6 K are shown in Fig. 1(e), for the case when we resonantly excited the $Al_{0.15}Ga_{0.85}As$ barrier surrounding the NDs using σ^+ circularly polarized light pulses. This optical excitation using circular polarization generates spin-polarized electron-hole pairs due to the optical selection rule, which takes the angular momenta of the electrons and holes and the circular polarization of the light into account.[22] The PL spectra of an 8 nm-thick GaAs QW, which was grown on the same substrate wafer as these NDs under identical growth conditions, are also shown for the same circularly polarized excitation as a reference sample. The peak PL wavelength of the GaAs ND ensemble is 780 nm, which is clearly blue-shifted from that of the GaAs QW (804 nm) due to lateral quantum-confinement effects. The linewidth of the

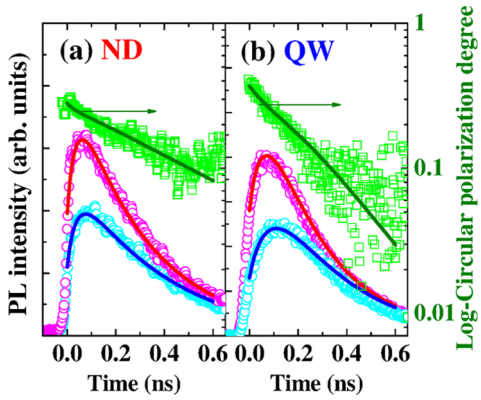

FIG. 2. Circularly polarized PL time-profiles (red open circles: σ^+, blue open circles: σ^-) and the CPD as a function of time (green open squares) at 6 K in (a) the GaAs NDs with the PL-wavelength range of 775-785 nm and (b) the reference GaAs QW with the PL-wavelength range of 800-805 nm, under σ^+-polarized pulsed excitation with the excitation power of 5 mW. Solid lines are best-fit calculations of the rate equation analysis reflecting the exciton-spin relaxation times.

GaAs-ND emission can be attributed to the distribution of the ND diameters shown in Fig. 1(c). We calculated the exciton energy confined within these NDs, taking this size distribution into account. This simulated exciton-PL spectrum, plotted in Fig. 1(d), agrees fairly well with the observed PL spectrum. The difference in the PL intensity between σ^+ (co-circular) and σ^- (counter-circular) is clearly observed for both the ND and QW emission. Here, the degree of the circular polarization (CPD) of the PL was defined as $(I_\sigma^+ - I_\sigma^-)(I_\sigma^+ + I_\sigma^-)$, with circularly polarized PL intensities (I_σ^+, I_σ^-). The CPD values are also plotted as a function of wavelength in Fig. 1(e). In the ND-PL, about 20% of the CPD is obtained around the peak wavelength of the PL spectrum. This strong co-circular property of the PL for the excitation polarization is indicative of an injection of spin-polarized carriers from the barrier and spin-selective recombination prior to the spin relaxation in the NDs, as will be confirmed by observing the time-resolved PL, discussed below.

Time profiles of the circularly polarized PL intensities in the GaAs NDs after σ^+ excitation, with a wavelength window of 775-785 nm for the PL spectra, are shown in Fig. 2(a). The PL intensities increase rapidly after the pulsed excitation, corresponding to the carrier injection from the barrier, then decrease exponentially due to the radiative recombination of excitons or non-radiative relaxation to dark-exciton states. Immediately after the pulsed excitation, the difference in the PL intensities between the σ^+– and σ^-–components is at its maximum, and this difference reduces with time. The time profile of the corresponding CPD, which is not only contributed from the exciton-spin relaxation within the GaAs NDs but also the state-filling-induced initial drop-off of CPD after the spin-polarized carrier injection,[23] is also plotted in Fig. 2(a). We analyzed the decay profiles of the circularly polarized PL using the rate equations, including the injection and relaxation processes of the spin-polarized excitons initially generated in the barrier and the state-filling at the ND states.[23] By this model, we can distinguish the state filling phenomena from the spin-relaxation time.

In Fig. 2(a), solid lines are the calculated best fits of these rate equations. From this fitting, the exciton-spin relaxation time (τ_s) is deduced to be 1.40 ns at 6 K. We performed the same measurement for the original GaAs QW grown on the same substrate, as shown in Fig. 2(b). τ_s of 0.44 ns is obtained from the same fitting, which is significantly shorter than that obtained from the NDs. Specifically, τ_s in the GaAs NDs is more than three times longer than that of the original GaAs QW prior to the ND formation.

The spin-relaxation times of the GaAs NDs and the QW are plotted as a function of excitation power (P) in Fig. 3(a). In the case of the QW, τ_s decreases monotonically as the P increases. For the exciton-spin relaxation in GaAs QWs, it has been reported that at low temperatures the Bir-Alnov-Pikus (BAP) mechanism[24] is dominant. In this mechanism, an exchange interaction between an electron and a hh can enhance the electron-spin and thus the exciton-spin relaxation

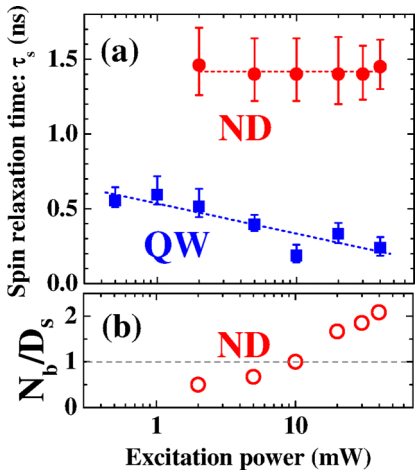

FIG. 3. (a) Excitation-power dependence of the spin-relaxation time (τ_s) at 6 K in the GaAs NDs (red filled circles) and in the original QW (blue filled squares). Dashed lines are included as a guide for the eyes. (b) The saturation factor N_b/D_s (red open circles) obtained from the rate equation analysis for GaAs NDs as a function of excitation power. The dashed line is a guide to indicate the level of the state-filling effect in the NDs.

as a result of the unstable hh-spin state that arises from the substantial mixing of states with different angular momenta. When the BAP mechanism is dominant, τ_s monotonically decreases with increasing P, as we observed here, due to an increase in the effective hh concentration versus that of the electrons. In contrast, in the GaAs NDs, τ_s is much longer than that in the QW, and are not dependent on the P. The density of injected excitons into the NDs can be evaluated from the P-dependence of the state-filling, obtained from our rate equation analysis. In Fig. 3(b) we have plotted the parameter N_b/D_s as the saturation factor; a ratio between the initial number of spin-polarized exciton generated in the barrier (N_b) and the density of the spin-polarized state in the NDs (D_s).[23] This saturation factor is equal to one when each ND is fully occupied by one exciton, and becomes larger than one when more excitons are injected, for example, in the excited states of the ND or by the formation of exciton molecules. Therefore, we see that the spin-relaxation time in the NDs is not affected by the number of excitons in the ND, i.e., by the strength of the effective field of the hh exchange interaction for the electron spin, even though more than one exciton exists in each ND above P = 10 mW as experimentally shown in Fig. 3(b).

Fig. 4 shows the temperature (T) dependences of τ_s in the GaAs NDs and the reference QW, where we compare the ND samples with different thicknesses of 8 and 4 nm. In the case of the QW, the T-dependence is similar to that previously reported for a GaAs QW.[12,14,15] τ_s is almost constant in the low T region below 40 K, which indicates that the BAP mechanism is dominant due to exciton formation. τ_s starts to decrease above 40 K and then shows a $T^{-0.9}$–dependence as shown in the figure inset, which is characteristic of the D'yakonov-Perel' (DP) mechanism[25] for electron-spin relaxation in the GaAs QW. Scattering of the electrons by impurities and defects in the QW can induce momentum and energy relaxation among different spin-split subbands originating from spin-orbit interactions in a zinc-blend (100) lattice structure. In contrast, τ_s in the NDs decreases as the temperature rises, even in the lowest T region. Generally, the exciton binding energy in NDs should be markedly larger than that in the QW and the resultant dissociation temperature of the excitons in the NDs can be significantly higher than that in the QW. If the BAP spin-relaxation mechanism is dominant in the NDs, τ_s will be constant up to the exciton dissociation temperature, which is higher than the 40 K observed in the original QW. However, the experimental trend for τ_s in the low T region is quite different; it starts to decrease from a temperature as low as 10 K. Therefore, the BAP induced exciton-spin relaxation is not dominant in this ND system.

This T-dependence can be understood as resulting from a thermal-excitation process among different spin states of the exciton, as was previously found in self-assembled InAs QDs.[6] We fit the

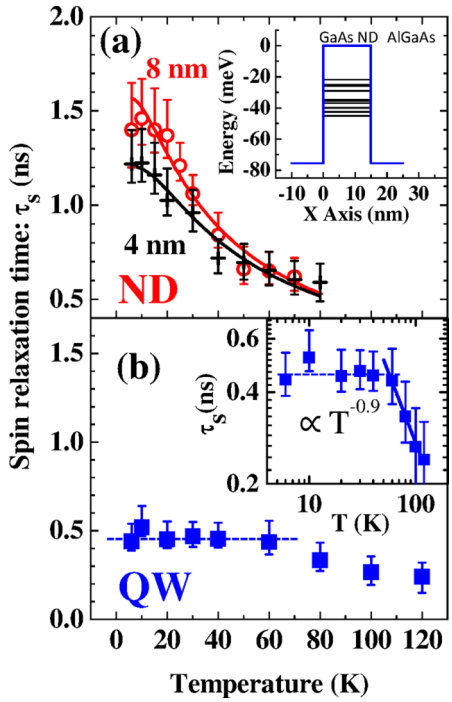

FIG. 4. Temperature dependence of τ_s in (a) the 8 nm-thick GaAs NDs (red open circles), 4 nm-thick GaAs NDs (black crosses) and (b) the 8 nm-thick QW (blue filled squares). The red and black solid lines for the NDs indicate calculations taking thermal activation energies into account. The inset of (a) shows the calculated valence band structure and eigenvalues of hole states for the 8 nm-thick NDs. The blue dashed line for the QW is a guide for the eyes. The inset of (b) shows a log-scale plot of the data for the QW, and the solid line indicates the $T^{-0.9}$–dependence.

T-dependence of τ_s using the following equation:

$$\frac{1}{\tau_s} \propto 1 + \frac{1}{\exp(E/kT) - 1},$$

assuming that the spin-relaxation rate is proportional to the scattering rate of acoustic phonons and E_{act} is the activation energy in the spin-relaxation process. E_{act} is obtained to be 3.9 meV for the thinner 4 nm-thick NDs, which is clearly larger than 2.8 meV for the 8 nm-thick NDs. Three-dimensional $k \cdot p$-band calculation results for the hole states based on the present disk shape, with the diameter of 15 nm, thickness of 8 or 4 nm, and embedded in the $Al_{0.15}Ga_{0.85}As$ barrier are summarized in Table I. The energy differences between the ground state and the first-excited state are calculated to be 3.2 meV (8 nm) and 5.0 meV (4 nm) which depend on the degree of quantum confinement (disk thickness), and they are fairly close to the experimentally deduced E_{act} for the exciton-spin relaxation. The degree of the hole state mixing, which is shown as the composition of light hole (lh) and hh wavefunctions in Table I, is different between the ground and the first-excited state.

TABLE I. Calculated confinement energies of the ground (E_{h1}) and first-excited (E_{h2}) hole states in the GaAs NDs with the diameter of 15 nm and thickness of 8 or 4 nm. The mixing ratio between the hh and lh wavefunctions is also shown. The energy difference (ΔE) between the calculated E_{h1} and E_{h2}, and the experimental thermal activation energy (E_{act}) for the spin-relaxation are also listed.

Thickness	**8 nm**	**4 nm**
$\mathbf{E_{h1}}$ (meV)	21.7 (hh: 88%, lh: 12%)	35.7 (hh: 91%, lh: 9%)
$\mathbf{E_{h2}}$ (meV)	25.0 (hh: 46%, lh: 54%)	40.7 (hh: 56%, lh: 44%)
$\mathbf{\Delta E_{h1}}$ (meV)	3.2	5.0
$\mathbf{E_{act}}$ (meV)	2.8	3.9

In other words, the angular momenta of these ground and first-excited hole states are significantly different. Therefore, the thermal excitation from the ground state into the first-excited state of the hole caused by the absorption of acoustic phonons can induce exciton-spin relaxation via the exchange interaction between the hole and electron wavefunctions. Furthermore, an elastic exciton-scattering process involving two consecutive phonons (phonon absorption and emission) can contribute to this spin relaxation.[7] τ_s will also decrease with increasing temperature in this process. Moreover, τ_s at the low-temperature limit around 4 K depends on the ND thickness. The mixing of hh and lh components at the lowest hole state is almost identical between these samples as shown in the Table I. In our NDs, exchange effects due to in-plane shape anisotropy can be ruled out because of the symmetrical disk shape in addition to potential formation of positive trions originating from naturally doped carbon-related acceptors commonly seen in the MOVPE process. A convincing explanation of this disk-thickness dependence of τ_s is an effect of the hyperfine interaction of nuclear spins in the NDs.[26,27] The degree of the dynamic nuclear polarization induced by spin-polarized electrons can be affected by the degree of quantum confinement because the hyperfine interaction strength depends on coupling strength of the electron wavefunction with an ensemble of nuclear spins. On the other hand, the stronger coupling can also induce energetic splitting of the electron level and the nuclear polarization saturates. Therefore, the effect of the degree of quantum confinement on the spin-relaxation time due to the dynamic nuclear polarization needs further investigation.

The effects of artificial strong lateral quantum confinement on the exciton-spin relaxation dynamics have been studied in GaAs NDs with a lateral diameter of 15 nm. Time-resolved circularly polarized PL from the NDs indicates strong suppression of the exciton-spin relaxation, changing from 0.44 ns in the original QW prior to ND fabrication to 1.40 ns in the NDs at 6 K. The spin-relaxation time of the GaAs NDs is insensitive to the excitation power and systematically decreases with increasing temperature, which indicates that the exciton-spin relaxation in the NDs originates from thermal excitation among the hole states with different angular momenta.

ACKNOWLEDGMENT

This work is supported in part by the Japan Society for the Promotion of Science (JSPS), Grant-in-Aid for Scientific Research (S) No. 22221007.

[1] K. M. Weiss, J. Miguel-Sanchez, and J. M. Elzerman, Sci. Rep. **3** (2013).
[2] G. Wang, B. L. Liu, A. Balocchi, P. Renucci, C. R. Zhu, T. Amand, C. Fontaine, and X. Marie, Nat. Commun. **4** (2013).
[3] D. D. Awschalom and M. E. Flatte, Nat. Phys. **3**, 153 (2007).
[4] M. Kroutvar, Y. Ducommun, D. Heiss, M. Bichler, D. Schuh, G. Abstreiter, and J. J. Finley, Nature **432**, 81 (2004).
[5] J. M. Elzerman, R. Hanson, L. H. Willems van Beveren, B. Witkamp, L. M. K. Vandersypen, and L. P. Kouwenhoven, Nature **430**, 431 (2004).
[6] A. Tackeuchi, R. Ohtsubo, K. Yamaguchi, M. Murayama, T. Kitamura, T. Kuroda, and T. Takagahara, Appl. Phys. Lett. **84**, 3576 (2004).
[7] H. Gotoh, H. Kamada, H. Ando, and J. Temmyo, Jpn. J. Appl. Phys. **42**, 3340 (2003).
[8] D. Dagnelund, I. A. Buyanova, W. M. Chen, A. Murayama, T. Furuta, K. Hyomi, I. Souma, and Y. Oka, Phys. Rev. B **77**, 035437 (2008).
[9] A. Murayama, T. Furuta, K. Hyomi, I. Souma, Y. Oka, D. Dagnelund, I. A. Buyanova, and W. M. Chen, Phys. Rev. B **75**, 195308 (2007).
[10] S. Mackowski, T. Gurung, H. E. Jackson, L. M. Smith, W. Heiss, J. Kossut, and G. Karczewski, Appl. Phys. Lett. **86**, 103101 (2005).
[11] A. Tackeuchi, T. Kuroda, S. Muto, Y. Nishikawa, and O. Wada, Jpn. J. Appl. Phys. **38**, 4680 (1999).
[12] A. Tackeuchi, Y. Nishikawa, and O. Wada, Appl. Phys. Lett. **68**, 797 (1996).
[13] M. Z. Maialle, E. A. de Andrada e Silva, and L. J. Sham, Phys. Rev. B **47**, 15776 (1993).
[14] A. Vinattieri, J. Shah, T. C. Damen, K. W. Goossen, L. N. Pfeiffer, M. Z. Maialle, and L. J. Sham, Appl. Phys. Lett. **63**, 3164 (1993).
[15] J. Wagner, H. Schneider, D. Richards, A. Fischer, and K. Ploog, Phys. Rev. B **47**, 4786 (1993).
[16] Y. Tamura, T. Kaizu, T. Kiba, M. Igarashi, R. Tsukamoto, A. Higo, W. Hu, C. Thomas, M. E. Fauzi, T. Hoshii, I. Yamashita, Y. Okada, A. Murayama, and S. Samukawa, Nanotechnology **24**, 285301 (2013).
[17] T. Kaizu, Y. Tamura, M. Igarashi, W. Hu, R. Tsukamoto, I. Yamashita, S. Samukawa, and Y. Okada, Appl. Phys. Lett. **101**, 113108 (2012).
[18] X.-Y. Wang, C.-H. Huang, R. Tsukamoto, P.-A. Mortemousque, K. M. Itoh, Y. Ohno, and S. Samukawa, Nanotechnology **22**, 365301 (2011).
[19] S. Samukawa, Jpn. J. Appl. Phys. **45**, 2395 (2006).
[20] I. Yamashita, Thin Solid Films **393**, 12 (2001).

[21] R. Tsukamoto, M. Godonoga, R. Matsuyama, M. Igarashi, J. G. Heddle, S. Samukawa, and I. Yamashita, Langmuir **29**, 12737 (2013).
[22] F. Meier and B. Zakharchenya, *Optical Orientation* (North-Holland, Amsterdam, 1984).
[23] T. Kiba, X.-j. Yang, T. Yamamura, Y. Kuno, A. Subagyo, K. Sueoka, and A. Murayama, Appl. Phys. Lett. **103**, 082405 (2013).
[24] G. L. Bir, A. G. Aronov, and G. E. Pikus, Sov. Phys. JETP **42**, 705 (1976).
[25] M. I. D'yakonov and V. Y. Kachorovski, Sov. Phys. Semicond. **20**, 110 (1986).
[26] P. F. Braun, X. Marie, L. Lombez, B. Urbaszek, T. Amand, P. Renucci, V. K. Kalevich, K. V. Kavokin, O. Krebs, P. Voisin, and Y. Masumoto, Phys. Rev. Lett. **94**, 116601 (2005).
[27] J. Beyer, Y. Puttisong, I. A. Buyanova, S. Suraprapapich, C. W. Tu, and W. M. Chen, Appl. Phys. Lett. **100**, 143105 (2012).